UDC 621. 316. 933

ZINC OXIDE GAPLESS ARRESTER (FUJI "Z-TRAP")

Masaharu Namba
Ikuo Nagasawa
Michiaki Miyagawa

I. INTRODUCTION

With the expanding applications of semiconductors such as thyristors, transistors and IC's in recent years, there has been rapid progress in the elimination of movable parts and compactness in measuring, control and communication devices and power conversion equipment. Naturally, the aims are to save labor by increasing the reliability of the equipment and improving the maintenability but there is a tendency for drops in the current withstand and voltage withstand and it is hoped that a protection method for overcurrents and voltages will be established.

The Fuji "Z-trap" is an absorbor for lightning and switching surges. Conventionally, there are five types of elements for this kind of overvoltage protection; (i) SiC varistor, (ii) selenium surge absorber, (iii) Si varistor, iv) solid state elements such as the Zener diode and (v) gap discharge arresters. The solid state elements used are those with non-linear voltage-current characteristics (non-linear coefficient α appears at $I \propto V^{\alpha}$, $\alpha > 1$) and the current flowing in the element at high resistance when the voltage is lower than the normally used voltage is small. When an overvoltage is applied, the resistance suddenly drops and a large current is absorbed. However, since the (i) and (ii) elements do not have such a high non-linear coefficient, the limit voltage during surge absorption is high. For (iii) and (iv), the non-linear coefficient is very high but the surge absorption energy is small and since it is not easy to manufacture elements with high operating voltages, they are used for surge absorption only in low voltage circuits. Because (v) is of the gap type, the discharge is delayed, the limit voltage is rather high and the spark over voltage varies, which are all disadvantages.

The Fuji "Z-trap" is a sintered zinc oxide element which shows considerable improvement over the disadvantages of the former surge absorbers. An exterior view is shown in *Fig. 1*. Originally, the zinc oxide sintered element was a n-type semiconductor with a comparatively low resistance but when suitable metal oxides were added and sintered, insulation layers were formed in the granular borders of each of the crystalline granules of zinc oxide making up the sintered structure. These serve as a potential wall against the current and the electrical resistance of the sintered element become non-linear. As will be evident later, since the "Z-trap" is a sintered element, the effective sectional area in respect to the passing surge absorption current is very large when compared with the SiC-varistor in which the electrical resistance is formed mainly by point contact between the granules. Therefore, the surge absorption capacity is high. The voltage applied to the sintered element is apportioned by the granular boundary layers equal to the number of particles connected in series. Therefore, it is easy to obtain an element with a limit voltage higher than that of the Zener diode in which the total voltage burden is in one joint part.

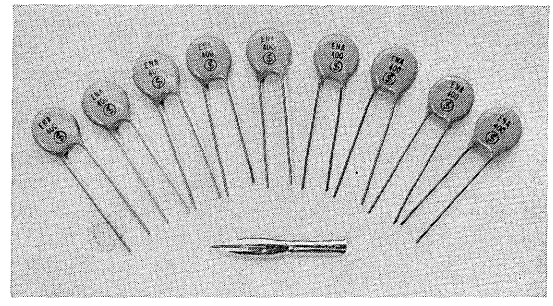

Fig. 1 Fuji "Z-trap"

The main advantages are as follows: (a) the voltage non-linearity is very high (the non-linearity coefficient is five times that of the SiC-varistor), (b) the leakage current is of the μA order or less, (c) the limit voltage is lower and more stable than in the varistors, (d) because of the rapid response to surges, surges in the form of a steep wave pulse can also be absorbed, etc. Unlike the selenium varistor, this element has basic positive/negative symmetrical voltage/current characteristics so that surge voltages from either the positive or negative polarity direction can be absorbed in the same way and the elements can be applied directly in either DC or AC circuits.

II. OPERATING PRINCIPLES

The main material of the Fuji "Z-trap" is zinc oxide which has a Wurtzite structure but since the zinc ion radius is smaller than the oxygen ion radius ($r_{Zn^2}/r_{O^2}=0.63$), it is easy for the zinc ions to enter the gaps in the lattice (Frenkel vacancy) and the zinc has a slight excess in the stoichiometric proportions of the oxygen and zinc atoms. The interstitial Zn atom (hereafter Zn (*i*)) dissociates at room temperature as follows so that ionization occurs and electrons are supplied in the conduction band.

$$Zn(i) \rightarrow Zn^+(i) + e^-$$

Therefore, the zinc oxide crystal shows n type semiconductor properties. When the metallic oxide (hereafter M_2O) of a monad such as Na_2O and Li_2O is added to the ZnO semiconductor and sintering is performed in the air, there is a substitution as follows of the Zn^{2+} and $2M^+$ in the crystal granules, the electron concentration drops and the electrical conductivity decreases.

$$ZnO\ \text{crystal} + M_2O \rightleftarrows 2M^+(Zn) - 2e^- + 2ZnO - \tfrac{1}{2}O_2\,(\text{gas})$$

$M^+(Zn)$ is the M ion in the normal lattice site of Zn. However, the reaction of ZnO in accordance with the decrease in free electrons,

$$ZnO \rightleftarrows Zn^+ + e^- + \tfrac{1}{2}O_2\,(\text{gas})$$

or

$$ZnO \rightleftarrows Zn^{2+} + 2e^- + \tfrac{1}{2}O_2\,(\text{gas})$$

proceeds to the right and the Zn^+ or Zn^{2+} increases. Since the rate of the material shift in the ZnO is determined by the interstitial Zn ion, the rate of sintering can be advanced by adding the M_2O.

Conversely, when a triad metallic oxide (hereafter M_2O_3) such as aluminum oxide or ferric oxide is added

$$ZnO\ \text{crystal} + M_2O_3 \rightleftarrows 2M^{3+}(Zn) + 2e^- + 2ZnO + \tfrac{1}{2}O_2\,(\text{gas})$$

occurs and the electrical conductivity increases. Because it is opposite from the M_2O case, the rate of granular growth becomes small. The same effects can also be obtained with silica and titanium oxide (MO_2) because of valency control.

The above additives not only do not contribute in any way to the non-linearity of the ZnO type resistors but are also actually harmful in the "Z-trap". The reason for this is that by mixing minute amounts of these substances, the elements might either gain a high resistance or a very low resistance and the effects of specific additives in promoting the non-linearity as described later is completely eliminated.

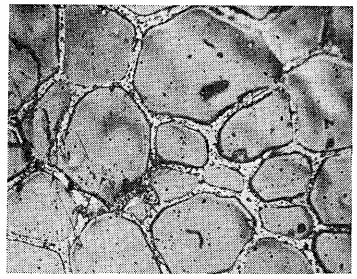

Fig. 2 Optical micrograph of sintered ZnO with La_2O_3–Co_3O_4 additives

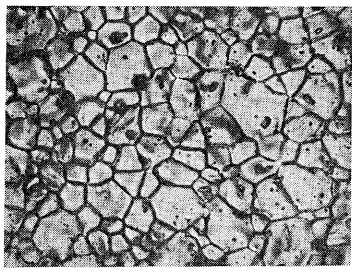

Fig. 3 Optical micrograph of sintered ZnO with Pr_6O_{11}–Co_3O_4 additives

The microstructure of the "Z-trap" sintered element as shown in *Figs. 2* and *3* consists of a boundary layer surrounding the segregate formed by the ZnO crystal granules. Since this boundary layer has a very high resistance compared with the ZnO crystal granules (specific resistance: several Ωcm), the voltage applied to the sintered element is almost all centered in the boundary layer. Because the thickness of the boundary layer is $0.1\sim1\,\mu$m in respect to a crystal granule diameter of $20\sim30\,\mu$m, the electric field of the boundary layer reaches $10^4\sim10^5$ and this strong field results in the same current rise phenomenon as with an electron avalanche. This can be considered as an element with non-linear electric resistance characteristics. Therefore, the "Z-trap" structually resembles the SiC-varistor most closely among the overvoltage absorption sold-state elements but it is completely different in respect to operation principles. The SiC varistor, generally speaking, is based on simple point contact of the SiC granules and the non-linear relation of the voltage and current is controlled by field radiation cur-

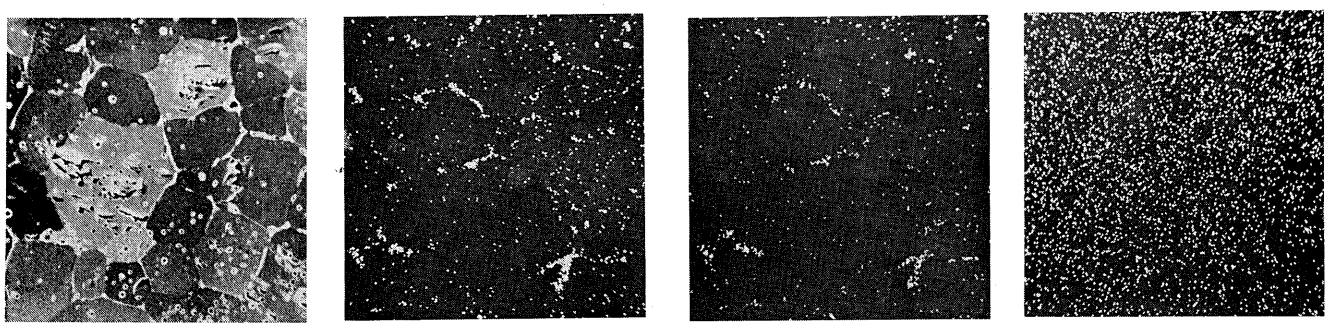

(a) secondary electron image (b) Pr-L_α X-rays image (c) La-L_α X-rays image (d) Co-K_α X-rays image

Fig. 4 Scanning electron microphotograph of sintered ZnO with Pr_6O_{11}–La_2O_3–Co_3O_4 additives

rent flowing in the spaces between mutually opposite granules. When considering the resistance due to this radiation current and the bulk resistance of the SiC inserted in series, the current of the SiC varistor basically stops in proportion to the 1.5～3 power (in relation to granule shape) of the applied voltage at the most.[2]

One method to form a high boundary resistance layer in the non-linear ZnO resistor is to add bismuth oxide (Bi_2O_3).[3] However, in the Fuji "Z-trap", rare earth oxides such as those of lanthanum (La_2O_3), praseodymium (Pr_6O_{11}) and terbium (Tb_4O_7) are used (patent applied for). La_2O_3 is a triad metallic oxide the same as Al_2O_3 but while the radius of the Al^{3+} ion is smaller than that of the Zn^{2+} ion, the radius of the La^{3+} ion is much larger so that the La is not dissolved in the ZnO but is segregated in the crystal boundary layer. The same is also the case for Pr_6O_{11} and Tb_6O_7. The non-linear characteristics are much greater than those when cobalt oxide (Co_3O_4) is added and the steep voltage/electrical characteristics are equal to those of the Zener diode. *Fig. 4(a)* shows observations with a scanning electron microscope of a ZnO sintered element with La_2O_3, Pr_6O_{11} and Co_3O_4 added. The section was etched by a dilute HCl solution but when the boundary layer part was analyzed with an X-ray spectroscope and the distribution of the various added elements were observed, the results were as in *Fig. 4(b)*, *(c)* and *(d)*. The Co distributed in the ZnO granules and was completed set but the La and Pr were segregated in the boundary area. From comparisons with *Figs. 2* and *3*, it is evident that the growth of crystal granules of ZnO including La_2O_3 is especially great. In the ESR measurement, part of the added La became La^{2+} and the increase in La^{2+} showed almost the same trend as crystal granule growth. Therefore, in the granular growth process when La was added, part of the La_2O_3 was dissolved in the granules as LaO under the high temperatures but the rest appeared in the boundary in relation to the ion radius of the La^{2+}. The O^{2-} remaining at that time combined with the uncoupled Zn^{2+} in the granules to form ZnO which resulted in granular growth. However, the LaO was not stable, scattered to the side where oxygen was present and returned to the form of La_2O_3. In the Fuji "Z-trap", La is added to elements for use in low voltage circuits such as DC 18V and DC 24V.

The behavior of Co is nor clear at present. The resistance of the sintered zinc drops to ⅓ by the addition of Co 0.1 at.% for example but the voltage dependence of the resistance does not appear only from the Co.

Therefore, Co is distributed uniformly in the ZnO crystal granules and acts as a donor but the most effective point of cobalt oxide as an additive is that it greatly improves the non-linear resistance as was mentioned previously. This is exactly the same when bismuth oxide is used instead of the rare earth elements[4] and the non-linear characteristics of the ZnO resistors without Co added are about the same as those of the SiC varistor. Because of its microstructure, it can be assumed that the sintered element has a rather high static capacity. The static capacity of the sintered element per unit area is given as follows for connection of the boundary layer and crystal granules in series.

$$C=\frac{d_1+d_2}{L}\cdot\frac{\varepsilon_1}{d_1}\fallingdotseq\frac{d_2}{d_1}\frac{\varepsilon_1}{L}$$

where L is the thickness of the sintered element, d_1 and ε_1 are the boundary layer thickness and dielectric constant respectively and d_2 and ε_2 are the crystal granule diameter and dielectric constant respectively. When $d_2/d_1\approx200$ and $\varepsilon_1\fallingdotseq\varepsilon_2$ (specific dielectric constant of ZnO crystal=8), the static capacity of an element with a thickness of 1 mm and a unit surface area (1 cm^2) is over 1,000 pF ($\approx200\times10^3\times8\times8.85\times10^{-12}\times10^{-4}$pF). By considering this static capacity, the element can be represented by the equivalent circuit shown in *Fig. 5*. Therefore, when an AC voltage is applied to the element a current proportional to this applied voltage flows because of the capacity admittance and compared with DC application, a much greater leak current is observed (refer to *Fig. 6*). However, the magnitude of this leak current is less than 100 μA and it presents no problem for normal use. *Fig. 7* shows a *v–t*, *i–t* oscillogram for the voltage/current characteristics in the low current range (mA order) and *Fig. 8* for the case when the maximum impulse current (100A order) is flowing.

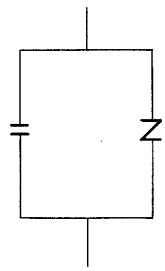

Fig. 5 Equivalent circuit for ZnO element

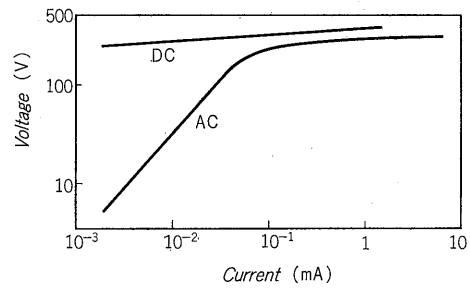

Fig. 6 DC and AC (50 Hz) leakage currents in ZnO element

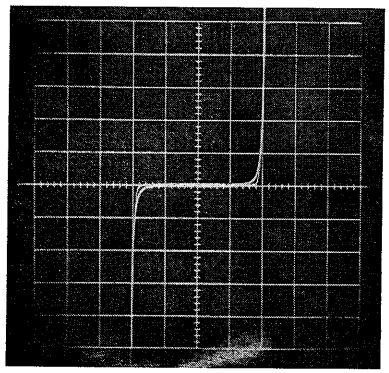

Fig. 7 Tipical *V–I* curve of ZnO element (Horiz. 100 V/div., vert. 5 mA/div.)

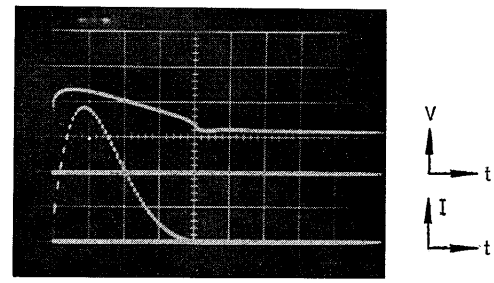

Fig. 8 Impulses *V–t* and *I–t* curve of ZnO element (Horiz. 10μs/div., vert. 200V/div. for *V–t* and 100A/div. for *I–t*)

Table 1 **Characteristics of Fuji "Z-trap"**

Type	ENA400-11	ENA850-11	ENA211-11	ENA211-12	ENA421-11	ENA421-12	ENA841-11	ENA841-12
Maximum permissible voltage	DC 20V	DC 27V	AC 120Vrms		AC 240Vrms		AC 480Vrms	
*Sparkover voltage (V_{1mA})	40V±15%	85V±15%	210V±15%		420V±15%		840V±15%	
*Residual voltage(8×20μs, 40A during conductive)	105V or less	200V or less	300V or less	375V or less	600V or less	750V or less	1,200V or less	1,500V or less
**Discharge withstand current rating(8×20μs wave)	2,000A	2,500A						
Rated frequency	DC		50Hz, 60Hz					
Ambient temperature	−40~+70°C	−40~+85°C						
Storage voltage	−40~+100°C							
External dimensions (t)	6.5mm max	7.5mm max	8.5mm max		9.5mm max		For 2 ENA421 types connected in series	

*Ambient temperature 25°C

**V_{1mA} charges of less than 10% at 2 conductings at a gap of about 2 min.

III. CHARACTERISTICS OF THE "Z-TRAP"

The following is an outlide of the method of manufacturing the Fuji "Z-trap". As was described previously, minute amounts of a rare earth oxide and cobalt oxide are added to ZnO powder and after shaping in suitable sizes, sintering is performed using the normal method of the ceramic industry. Then the sintered pellet is ground to the appropriate thickness according to requirements and after electrodes are fused to both sides, the lead wires are connected. A resin mold is added to finish the product.

The following sections introduce the types, ratings and typical limit voltage characteristics of Fuji "Z-traps".

Table 1 shows the guaranteed characteristics of the "Z-trap". The reason for selecting the value in respect to a 40A impulse current as the limit voltage is described in V. The spark over voltage (V_{1mA}) is defined as the terminal voltage when 1mA flows.

1. Residual Voltage Characteristics

As was mentioned previously, the voltage/current characteristics of this type of non-linear resistor are approximately $I \propto V^{\alpha}$. The non-linear coefficient α is closely connected to the voltage but when the voltages V_{1mA} and V_{10mA} for currents of 1mA and 10mA respectively are taken as standard for convenience, then

$$\alpha = 1/\log(V_{10mA}/V_{1mA})$$

The value of this is about 30 in the "Z-trap" compared with only 3~4 in the SiC varistor. *Fig. 6* shows the residual voltage characteristics for each series of "Z-traps". These measurements were made using DC in the current range under 100mA and a 8×20μs standard wave impulse current over 1A. As can be seen in the Tacle, the residual voltages in the ENA211-11 and ENA421-11 models for AC 100V and AC 200V when conducting a 40A impulse current were very low, less than 300 V and 600 V respectively. They are highly effective in the protection of semiconductors. *Fig. 10* shows the V_{1mA}

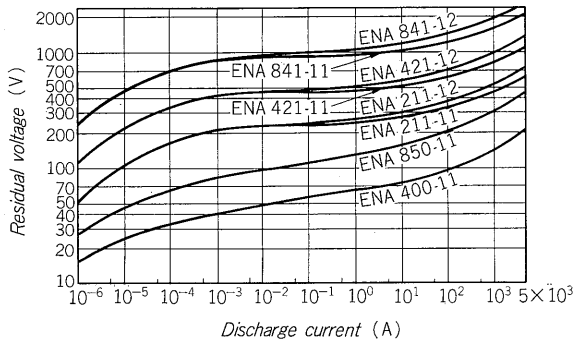

Fig. 9 Residual voltage-current characteristics of "Z-trap"

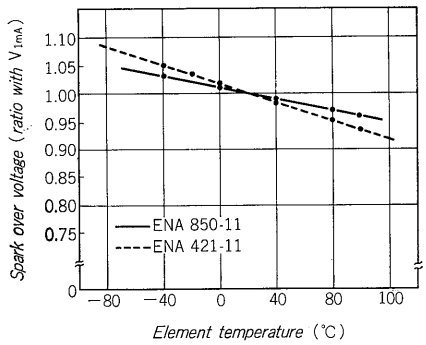

Fig. 10 Temperature dependence of V_{1mA} in Fuji "Z-trap"

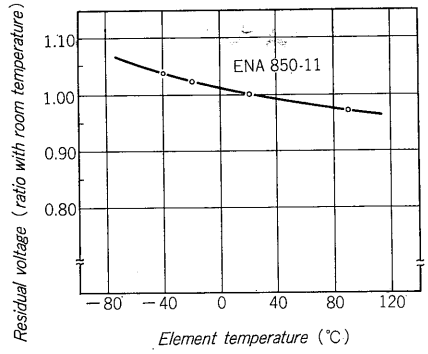

Fig. 11 Temperature dependence of residual voltage (for 40A impulse) in Fuji "Z-trap"

values (shown as a ratio with the V_{1mA} at the standard temperature of 20°C) for the ENA850–11 and ENA421–11 models and *Fig. 11* shows the temperature dependence characteristics of the residual voltage values (same as above) during flow of a 40A impulse current in the ENA850–11 in the −40 to 100°C range. The changes in the characteristics due to temperature were less than −0.1%/deg. which indicates high stability in respect to temperature changes.

2. Discharge Withstand

The element life is considered as the case after a discharge current of the standard waveform corresponding to the values for impulse (8×20μs) discharge withstand and the long wave tail (2ms, square wave) in JEC156 as well-known ratings for discharge withstand against lightning and switching surges, change rate in respect to the initial V_{1mA} reached 10% or more. The relation between the magnitudes of the discharge current and the number of applications is shown in *Figs. 12* and *13*. As a typical example for the ENA850–11, the withstand for the impulse discharge current is about 100 time at 2,000A and for the square wave current is about 200 times at 100A. Considering that the "Z-trap" is very compact as shown by the external dimensions in *Table 1*, it is evident that the element has a very large discharge withstand when compared with conventional elements. *Fig. 14* shows the relation between pulse width and discharge current magnitude

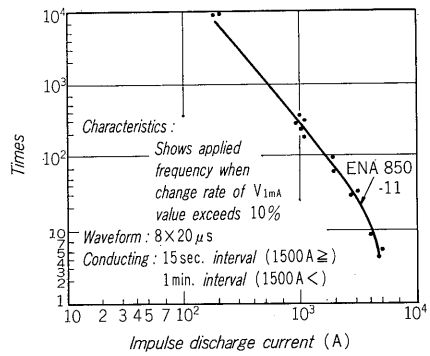

Fig. 12 Impulse duration current withstand in Fuji "Z-trap" (for waveform of 8×20μs)

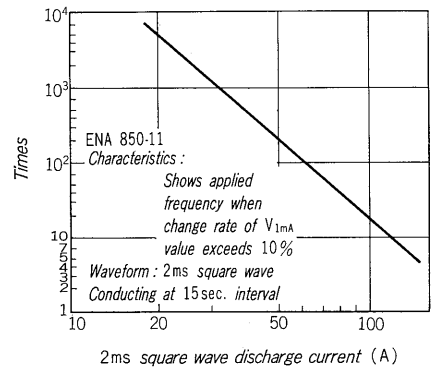

Fig. 13 Long duration current withstand in Fuji "Z-trap" (for 2 ms rectangular wave)

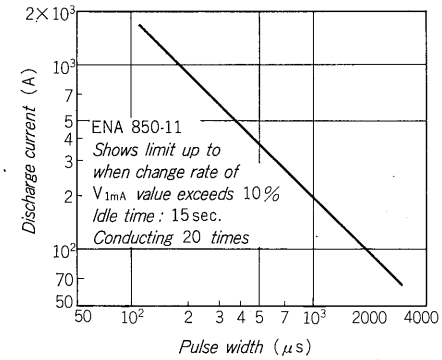

Fig. 14 Pulse width dependence of discharge current withstand in Fuji "Z-trap"

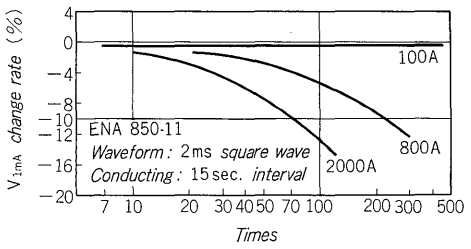

Fig. 15 Life vs. magnitude of 8×20μs discharge current relation in Fuji "Z-trap"

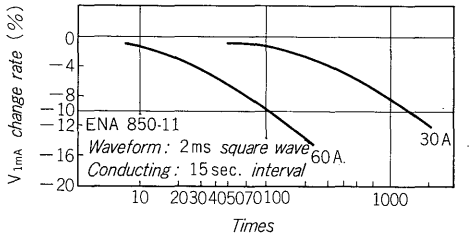

Fig. 16 Life vs. magnitude of 2ms rectangular discharge current relation in Fuji "Z-trap"

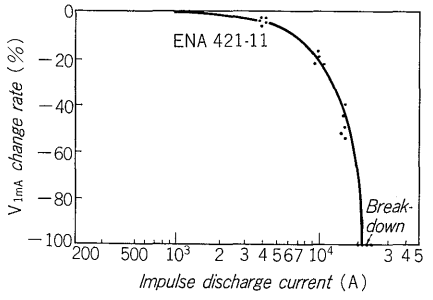

Fig. 17 Variation of V_{1mA} with the magnitude of 8×20μs discharge current

under conditions of 20 applications and V_{1mA} changes within 10%. *Figs. 15* and *16* show how the V_{1mA} changes in respect to number of applications with the discharge current as parameter for the impulse and square wave currents respectively.

Although it is not shown in the figure, the results of a case when the application was repeated many times were as follows. The change rate of the V_{1mA} in the ENA421-12 for 100A and an 8×20μs wave were withing 3% for 3,500 times and withing 10% for 10,000 times. This indicates that the "Z-trap" is very stable against repeated surges. *Fig. 17* shows the change rate of V_{1mA} when the impulse discharge current is applied once as a function of the discharge current. If the discharge withstand is as defined in the JEC Lightning Arrester Policies, the "Z-trap" can be said to have a withstand of more than 10,000A per 1cm².

3. Response Characteristics

Since the "Z-trap" does not have the time delay up to the start of discharge such as in the gap discharge arrester, response in respect to the input of a steep wave is rapid and the limit voltage increases by a few % even when an impulse current of a wave-front of 0.5μs is applied. Any surge can be followed. This is shown in *Fig. 18*.

4. Static Capacity

The static capacity of the "Z-trap" is over 1,000pF per cm² as was described in section II. Therefore, it is necessary to take sufficient precautions when using in hamonic or signal circuits. *Fig. 19* shows the frequency characteristics of the static capacity of the "Z-trap".

IV. "Z-TRAP" RELIABILITY

Since the "Z-trap" is used for overvoltage protection in various types of devices, both reliability and operating stability are essential. Fuji Electric has confirmed the ratings and characteristics of the "Z-traps" by means of tests concerning spark over voltage, leak current, residual voltage, dv/dt withstand, discharge withstand, etc. as was described in section III and through withstand deterioration tests and mechanical strength tests, it has been found that arrestor action is good under the handling and environmental conditions which could normally be encountered. Therefore, it has been shown that "Z-traps" have sufficient reliability for various types of applications. Examples of results of the reliability

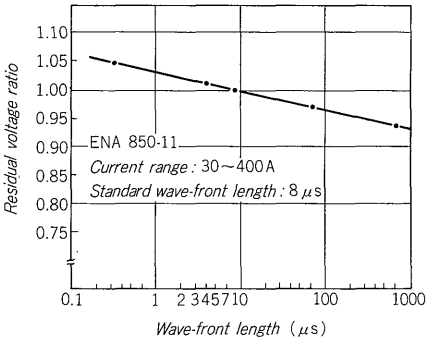

Fig. 18 Residual voltage-wave front steepness of applied voltage relation in Fuji "Z-trap"

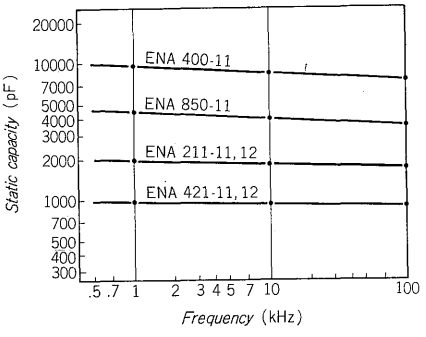

Fig. 19 Capacitance-frequency characteristics of Fuji "Z-trap"

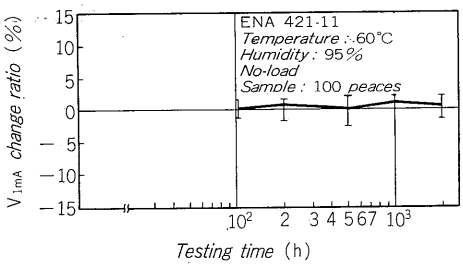

Fig. 20 Humidity-proof test (at no load)

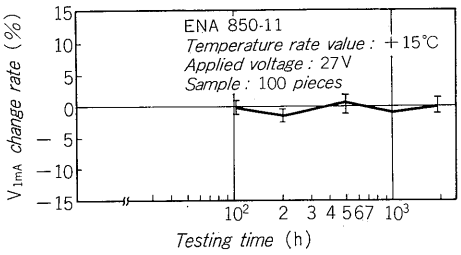

Fig. 21 High temperature test (at on load)

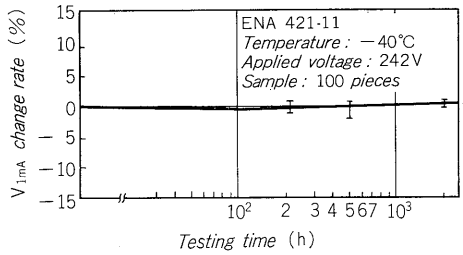

Fig. 22 Low temperature test (at on load)

tests are shown in *Figs. 20, 21* and *22* and in *Tabls 2* and *3*.

V. APPLICATIONS

1. Application Concepts

The points to be considered in the application of the "Z-traps" can be said to be the same as those for other surge absorbers but in general, the following three points must be investigated.

1) Coordination between the withstand voltage of the protected device and the residual voltage of the "Z-trap".
2) Coordination between the energy of the surge to be absorbed and the discharge withstand of the "Z-trap".
3) Problem points inherent in application circuits.

Some considerations are given below concerning points 1) and 2).

(1) Lightning surge protection

Fig. 23 shows the general circuit for application of the "Z-trap". When the forward wave voltage e_0 enters, the "Z-trap" current i_Z is given as follows:

$$i_Z=\frac{2e_0-e_Z(1+Z_1/Z_2)}{Z_1} \quad \text{.....(1)}$$

where e_Z : "Z-trap" residual voltage and Z_1 and Z_2 : circuit surge impedance.

As can be seen in *Fig. 24*, the intersection point P of the "Z-trap" e_Z-i_Z characteristics curve (1) and the circuit impedance characteristics curve (2) is the "Z-trap" discharge current and residual voltage at that time. In the worst case when $Z_2=\infty$, it is possible to consider $e_Z \ll 2e_0$ in the low voltage circuit and in practice, equation (1) can be expressed as follows:

$$i_Z \fallingdotseq \frac{2e_0}{Z_1} \quad \text{.....(2)}$$

The surge which arises in the low voltage circuit system consists in more than 90% of the cases of surges under 6 kV and if Z_1 is 300 Ω considering overhead wires, the discharge current of the "Z-trap" i_Z is as follows: $i_Z=2\times 6{,}000/300=40\text{A}$

In the cable system, the surge impedance Z_C becomes 20–200 Ω but since the transmission wave to the cable is $Z_C/(Z_1+Z_C)$ in respect to the penetration wave, the discharge current is the same as in the case of the overhead wires.

Therefore, if the insulation coordination with the standard discharge current of 40A in the low voltage system is considered, protection from the majority of lightning surges can be assured. This is also the reason why the value at a discharge current of 40A is shown in *Table 1* as the limit voltage for the "Z-trap".

(2) Switching surge protection

A standard example of the abnormal voltage which causes circuit switching is in the case of no

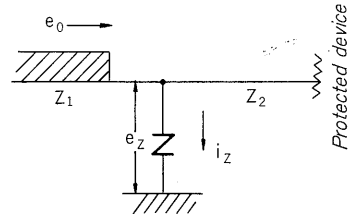

e_0 : penetration source wave
e_z : limit voltage of "Z-trap"
i_z : discharge voltage of "Z-trap"
Z_1, Z_2 : circuit surge impedance

Fig. 23 Surge protection circuit

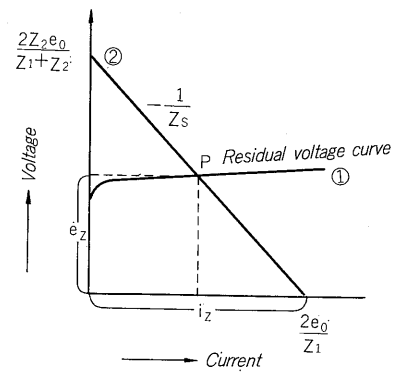

Fig. 24 Surge limiting operation of arrester

Table 2 **Environmental test items**

No.	Item	Test method	Example of characteristics
1	Temperature cycle test	A low temperature bath adjusted to −40°C and a high temperature bath adjusted to +100°C were prepared. The Z-traps were placed in the low temperature bath for 30 min., taken out and let stand at room temperature for 30 min., placed in the high temperature bath for 30 min. and then removed and let stand at room temperature for 15 min. With the above constituting one cycle, 5 cycles were repeated and finally, the samples were let stand for more than 1 hour but less than 2 hours. Than the operation starting voltage was measured. The test was passed when the changes were within ±10% and thered was no mechanical damage.	Changes of V_{1mA} within ±1%
2	Heat impulse test	After standing in 0°C water for 5 min., the samples were placed immediately in 100°C water for 5 min. and then placed immediately in the 0°C water. With this constituting one cycle, 5 cycles were repeated, the samples were allowed to stand for more than 1 hour and measurements were made. Comparisons were made with characteristics before the test and the test was considered as passed when changes in the operating starting voltage was within ±10% and there were no mechanical damages.	Changes of V_{1mA} within ±1%
3	Solder immersion test	The lowest 3 mm of the lead wires were immersed in molten solder at 260°C for 10 sec. and measurements were made at normal temperature of operation starting voltage, and changes in leak current and limit voltage. Comparisons were made with pretest characteristics and the test was considered passed if the changes were within ±10% and there were no mechanical damages.	Changes of V_{1mA} within ±1%
4	Solder adhesion test	The lead wires were immersed in molten solder at 200°C for 5 sec., the solder adhesion condition was investigated and if there were no abnormalities, the test was considered as passed.	No abnormalities
5	Boiling test	The samples were let stand for 5 hrs. in boiling water at 100°C, than jet stand for more than 1 hour at room temperature and the characteristics were measured. Characteristics before the test were compared and if the changes in operation starting voltage were within ±10% and there was no mechanical damage, the test was considered as passed.	Changes of V_{1mA} within ±1%
6	Humidity withstand test	The samples were kept in an environment of 60°C temperature and 95% humidity for more than 1,000hours and the time changes in operation starting voltage were investigated. Comparisons were made with before the test and the test was considered as passed if the changes were within ±10% and there were no mechanical damages.	Fig. 20
7	High temperature load test	The samples were let stand in a low temperature bath at−40°C for over 1,000 hours with the rate voltage applied and changes with time in the operation starting voltage were investigated. The test was considered as passed when changes in the above characteristics before, during and after the test were within ±10% and there were no mechanical damages.	Fig. 21
8	Low temperature load test	The samples were let stand for more than 1,000 hours in a low temperature water bath at −40°C with the rate voltage applied, The time changes in the operation starting voltage were investigated. If the changes before, during and after the test were within ±10% and there were no mechanical damages, the test was considered as passed.	Fig. 22
9	Standing test	(1) The sample was let stand for 1,000 hours in a high temperature bath at 100°C with no voltage. (2) The sample was let stand for 1,000 hours in a low temperature bath at −40°C with no voltage. The test was considered as passed if the operation starting voltage changes were within ±10% and there were no mechanical damages.	V_{1mA} changes within 3% and 2% respectively.

Table 3 **Mechanical strength test items**

No.	Item	Test method	Examples of characteristics
10	Vibration test	Lead wired of length 10 mm were selected and they were soldered to a suitable support terminal installed on the vibration plate. Vibrations of a frequency range of 10–50 Hz and a total amplitude of 1.5mm were applied at frequency steps of 10Hz→55Hz→10Hz at intervals of about 1 min. This was repeated. The vibrations were applied for a total of 6 hrs., 2 hrs. in each of the directions X, Y and Z. The test was considered as passed if the operation starting voltage changes were within ±10% and there were no mechanical damages.	V_{1mA} changes within ±1%
11	Drop test	The sample was dropped from a height of 75cm on an oak board of over 10mm in thickness and a total of 6 drops were performed, 2 each in the X, Y and Z directions. The test was considered as passed if the operation starting voltage changes were within ±10% and there were no mechanical dameges.	V_{1mA} changes within ±10%
12	Lead wire fatigue test	The body of the lead wires were hel so that the normalpulling axis was prependicular, a 0.5 kg hanging weight was suspended and after bending at 90°, the wire was returned to the original position. After bending in the opposite direction again at 90°C, the wire was again returned to the original position. This was repeated and the test was considered passed if the lead wires did not break.	No abnormalities
13	Terminal strength test	Suspention weights up to 1 kg were added gradually to the axial direction of the lead terminal and maintained for 1–5 sec. The test was considered as passed when there was no breakage.	No abnormalities

load switching in a transformer. The magnitude of the overvoltage at that time is determined by the magnitude of the excitation current and the breaker switching characteristics. When the "Z-trap" is operated at this overvoltage, the inductance energy at this switching current is absorbed and the overvoltage is surpressed. In the calculation of this absorbed energy, switching at the maximum value of the excitation current i_W considered as the worst case. At this time, the excitation energy W_{Tr} is as follows:

$$W_{Tr}=\frac{10\varepsilon P}{\omega} \quad \text{(when } 1\phi\text{)}$$

$$=\frac{5\varepsilon P}{\omega} \quad \text{(when } 3\phi\text{)}$$

P: rated capacity of transformer (kVA)
ω: angular frequency
ε: proportion of excitation current in rated current

The absorption energy W_Z of the "Z-trap" is decreased to about 1/2 of the W_{Tr} because of energy consumption and iron loss due to arcing and therefore, the "Z-trap" can be used in the range which satisfies the following relation:

$W_Z=1/2\ W_{Tr}$ "Z-trap" permissible absorption energy

The commutation current of the "Z-trap" can be considered as about 70% of the excitation current.

(3) Protection method when an especially low residual voltage is required

In electronic circuits, etc. where it is necessary to lower the residual voltage even when the "Z-trap" is used, it is possible to use either of the methods shown in *Fig. 25* (*a*) or (*b*). For the added impedance Z, either R or L can be considered but R is more desirable in the permissible range. When L is used, investigations are necessary concerning transmission of the slow wavefront of the transient oscillation voltage, switching surge, etc. due to floating C.

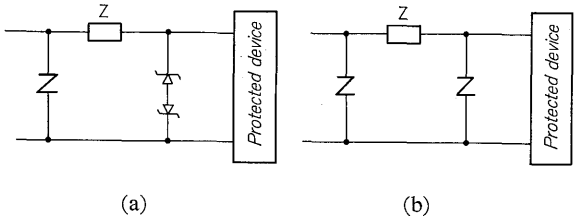

(a) (b)

Fig. 25 Circuit for low residual voltage

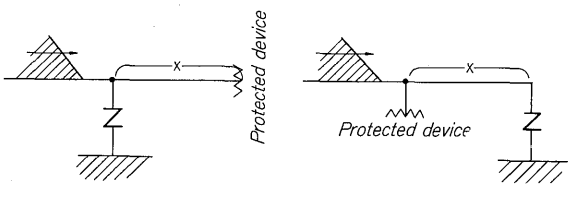

(a) (b)

Fig. 26 Fundamental protection circuits

(4) Separation from the protected device

When there is a separation of x (m) between the "Z-trap" and the protected device, the voltage increases in respect to the residual voltage e_Z of the "Z-trap".

In the case of *Fig. 26* (*a*) and (*b*), the voltage e_t applied to the protected device if the penetrating wave is a triangular wave can be obtained from the following equation:

$$e_t=e_Z+2\mu\cdot\frac{x}{v}\ \text{[kV]}$$

where,

v = surge advancing speed (300 m/s when overhead wires)

μ = wavefront steepness of penetrating wave (kV/μs)

Considering low voltage circuits, there is a voltage increase of 67 V/m even for $\mu=10$ kV/μs. Since the voltage tolerance in the low voltage circuit is small, it is desirable that the "Z-trap" and the protected device be directly coupled.

(5) Length of "Z-trap" lead wire

When steep wave currents flow in the "Z-trap" the lead wires act as an inductance and since the voltage $L\frac{di_Z}{dt}$ is added, it is necessary that the lead wires be a short as possible. This point is particularly important for low voltage circuits.

2. Examples of Applications

Two or three examples of the "Z-trap" will be described. *Fig. 27* (*a*) shows an example of applica-

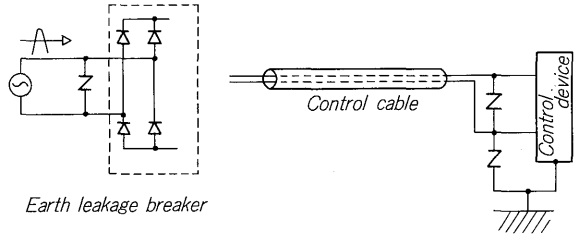

(a) Protection of earth leakage breaker (b) Protection of control device in substation

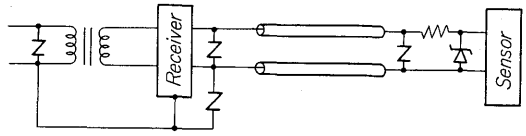

(c) Surge protection of fire warning system

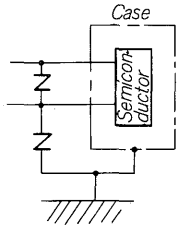

(d) General semiconductor protection

Fig. 27 Application examples of Fuji "Z-trap"

tion in a semiconductor leak breaker (ELB) but use of the "Z-trap" will greatly reduce the voltage withstand of diodes and other semiconductors. This method is widely used in rectifying circuits. *Fig. 27 (b)* shows an example of protection of a control device against abnormal voltages coming from low voltage control cables. *Fig. 27 (c)* is an example of surge protection in a fire alarm system. The normal protective circuit also often is for cases of very long cables. In the semiconductor protection shown in *Fig. 27 (d)*, it is necessary to insert the "Z-trap" in two places, between the poles and between 1 wire and ground (case). Particularly when it is necessary to reduce the limit voltage, the "Z-trap" can be inserted in the final stage for the method described in *(c)*.

The following are other applications of the Fuji "Z-trap":

Surge protection of low voltage distribution panels and distribution circuits (including domestic inlets)
Protection of distribution towers and against switching surges of low voltage motors
Surge protection of electronic devices and protection of railway signal equipment
Protection of road signal equipment and for street lightning
Protection of semiconductor converters and set voltage and current power sources
Protection of remote controlled measuring instruments and various types of semiconductor switches
Protection of relay station broadcasting equipment for radio, television, etc.
Surge absorption for various types of relays and electromagnetic switches
Peripheral equipment of computers

VI. CONCLUSION

Recently, "Z-trap" products have been introduced as surge absorbers with excellent voltage nonlinear characteristics. These elements have lower residual voltages, higher surge absorption capacities and greater stability against various environmental conditions than conventional varistors. In the future it is expected that the many features of these "Z-trap" will be confirmed and they will be widely used for surge protection of various devices and electronic circuits.

References:

(1) G. Heiland, E. Mollowo and F. Stöckmann: Solid state physics, Academic Press, p. 217 (1959)
(2) R.W. Sillars: Proc, Phys, Soc., **B68**, 881 (1955)
(3) M. Matsuoka: J.J.A.P. **10**, 736 (1971)
(4) Masuyama: Electronic Ceramics, **4**, 64 (1973)